THE ROYAL SOCIETY

Received 4 June 2001
Accepted 10 August 2001
Published online 10 December 2001

Limited-view iridescence in the butterfly *Ancyluris meliboeus*

P. Vukusic[1*], J. R. Sambles[1], C. R. Lawrence[2] and R. J. Wootton[3]

[1]*Thin Film Photonics, School of Physics, University of Exeter, Exeter EX4 4QL, UK*
[2]*Mechanical Sciences Sector, Signatures Group, QinetiQ, Farnborough, GU14 0LX, UK*
[3]*School of Biological Sciences, University of Exeter, Exeter EX4 4PS, UK*

Few mechanisms exist in nature that effect colour reflectivity, simultaneously high in spectral purity and in intensity, over a strictly limited portion of solid angle above a surface. Fewer still bring about such colour reflectivity with an angle dependence that is distinct from the colour transition associated with conventional multilayer interference. We have discovered that the ventral wings of the butterfly *Ancyluris meliboeus* exhibit these optical effects, and that they result from remarkable nano-scale architecture on the wing scales of the butterfly. This nano-structure is in the form of high-tilt multilayering that, as a result of abrupt termination of the multilayers, brings about diffraction concurrently with interference. The product is bright structural colour in a limited angular region over the ventral wing surface that enables remarkably strong flicker and colour contrast through minimal wing movement. The visibility effects associated with its colour, in terms of bright and dark zones of the observation hemisphere over the wing surface, are described. We suggest the purpose of the high-contrast ventral wing visibility associated with *A. meliboeus* is at-rest signalling; this is distinct from the dorsal wing visibility of other species such as those of the genus *Morpho*, the function of which is largely for in-flight signalling.

Keywords: structural colour; interference; multilayer; diffraction; butterfly

1. INTRODUCTION

Iridescent coloration is common in Lepidoptera and has been characterized for many different species (Lippert & Gentil 1959; Ghiradella *et al.* 1972; Huxley 1975). Such iridescence predominantly originates from optical interference within multilayer structures (Ghiradella 1991). These structures prove to be complex in their architecture and may be incorporated into configurations that can often produce several different optical effects (Vukusic *et al.* 2000*a*). Such effects include diffraction-assisted reflection angle broadening (Vukusic *et al.* 1999), all-structural colour mixing and strong polarization effects (Vukusic *et al.* 2000*b*).

Males of the riodinid butterfly *Ancyluris meliboeus* Fabricius produce a striking and unusual variety of iridescence only on the ventral side of their wings (DeVries 1997) (iridescence on most butterflies is usually found on the dorsal side of the wing). The colours that appear on each single iridescent wing region, at different wing orientations, range from deep blue through to orange. Few butterflies, if any, exhibit such a broad range of structural colour from a single region of wing.

The butterfly is also unusual because of the limited solid angle over the ventral side of the wing from which its iridescence is visible, even under diffuse illumination (Vukusic *et al.* 2001). The wing appears iridescent only from a restricted viewing perspective within its observation hemisphere. Outside this perspective there is no iridescence, and the wing appears black.

In this paper, we present the results of our investigation into the structural colour effects associated with *A. meliboeus*. We account for two effects. First, that the especially 'flashing' nature of its iridescence is a direct result of the tilt of its scale multilayering. Second, that the very broad range of reflected colours derives from the combined effect of interference and diffraction from its scale structure.

2. MATERIAL AND METHODS

Colour photography was used to demonstrate the colour effects described for this butterfly, a dead specimen of which was obtained from Worldwide Butterflies Ltd (Dorset, UK). Under diffuse illumination, one of its hind-wings was photographed through a series of wing tilts. In this way, the dependence of wing colour on viewing perspective could be recorded. Additionally, to show in one image the full range of strongly reflected colours, a collimated narrow beam of white light from a tungsten–halogen source was made incident onto one of the iridescent sections of wing. The reflection from this wing section was directed onto a flat white screen that was placed in front of the specimen and photographed. All photographs were taken using a Pentax LX camera with a Tamron 90 mm macro lens. Shutter speeds of *ca.* 30 s were used in conjunction with apertures set at between *f*5.6 and *f*11. Despite visual sensitivity at ultraviolet (UV) wavelengths associated with many butterfly species, spectroscopic measurements indicate that there is negligible UV reflectivity from these iridescent wing sections below 390–395 nm. Accordingly, further UV characterization was not pursued.

To determine the angular nature of the reflectivity from a single iridescent scale of *A. meliboeus*, a scale was removed from an appropriate section of its hind-wing and mounted, by its basal end, onto a ground-down needle tip. This single needle-mounted scale was positioned at the centre of an Euler cradle (Diffraction Technology, Canberra, Australia), its centre coincident with the path of a laser beam. In this way, and using a scanning photodiode detector, optical reflection and trans-

*Author for correspondence (p.vukusic@ex.ac.uk).

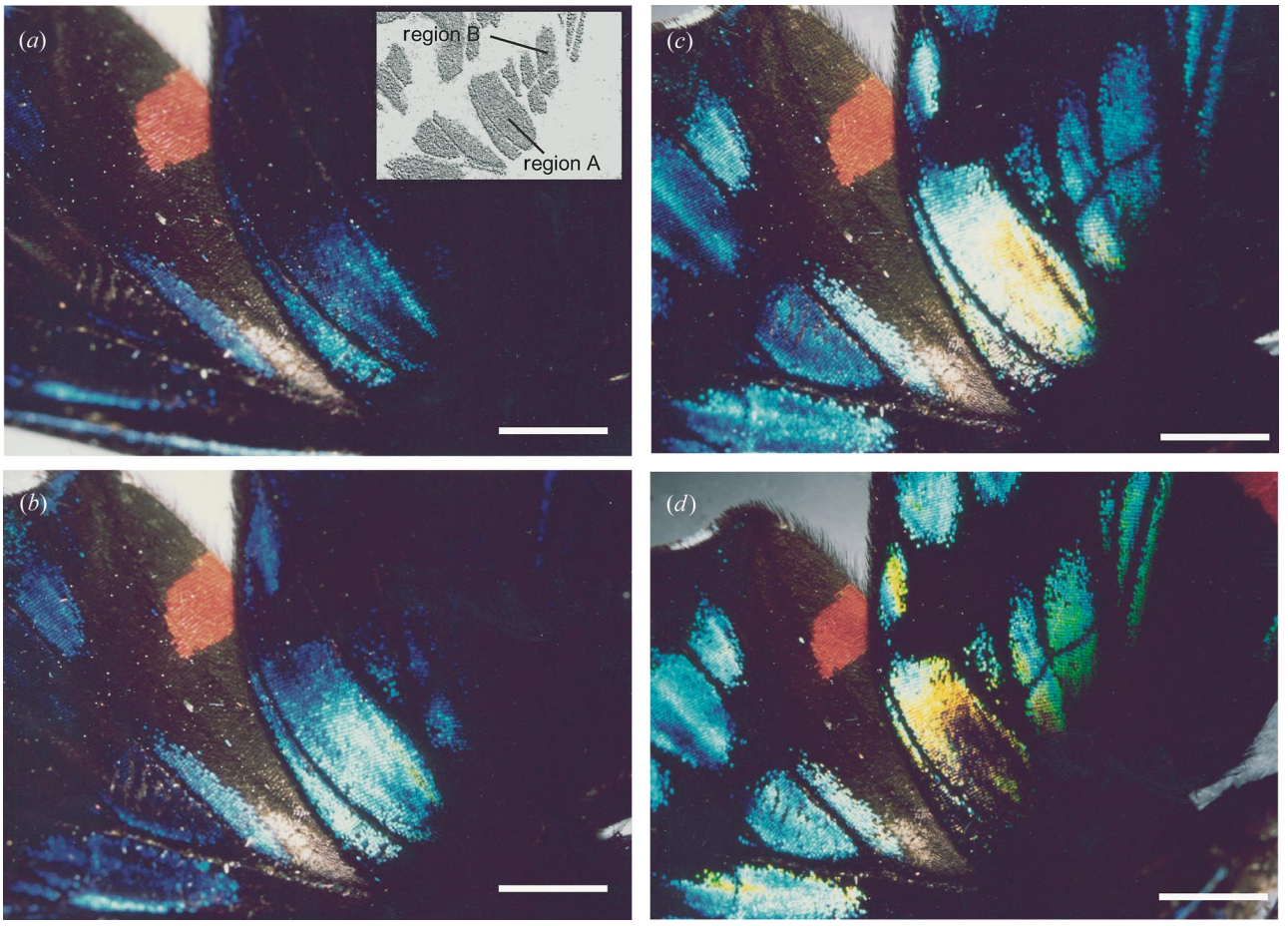

Figure 1. (*a–d*) Sequence of colour photographs of an *A. meliboeus* ventral hind-wing, taken during a series of wing tilts in 5° steps. (*a*) Inset picture: schematic map of the iridescent regions of the ventral hind-wing surface, all of which are iridescent in image (*c*). Scale bars, 3 mm.

mission data could be taken on the single scale at any chosen angle. Details of the method by which such single-scale data were collected is published elsewhere (Vukusic *et al.* 1999).

Full characterization of the scale structure of this butterfly required the use of electron microscopy—scanning electron microscopy (SEM) to obtain an image of the surfaces of the scales, and transmission electron microscopy (TEM) to obtain an image of the scale cross-sections. SEM images were taken using a Hitachi S-3200N electron microscope, after samples were coated with a 4 nm gold film. TEM images were taken after fixing wing samples in 3% glutaraldehyde at 21 °C for 2 h, followed by rinsing in sodium cacodylate buffer. The samples were then fixed in 1% osmic acid in buffer for 1 h followed by block staining in 2% aqueous uranyl acetate for 1 h, dehydration through an acetone series ending with 100% acetone and they were then embedded in Spurr resin. Post-microtomed sample sections were stained with lead citrate and examined using a JEOL 100S transmission electron microscope.

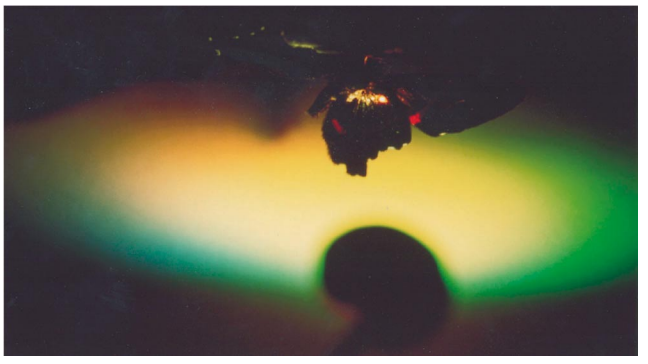

Figure 2. Real-colour photograph illustrating the range of hues produced from a single iridescent region of wing (region A from the inset picture in figure 1*a*). A narrow beam of collimated white light, incident normally on iridescent region A, produces this very broad range of colour, each one reflected at a slightly different angle.

3. RESULTS AND ANALYSIS

Figure 1 shows photographic images of a hind-wing of *A. meliboeus* under diffuse illumination as it is tilted over a small angle range in 5° steps. The inset to figure 1*a* is a schematic map of the iridescent regions of the hind-wing.

Inspection of these images illustrates several effects. Even within this limited range of wing tilt, region A is seen to iridesce over a broad range of colours. It changes from deep blue in figure 1*a*, to cyan in figure 1*b*, yellow-white in figure 1*c* and shows traces of orange in figure 1*d*. Images not presented here, starting before and ending after this sequence, show no iridescence appearing from this region. In these non-iridescent instances, wing orientation places the camera outside the limited portion of the observation hemisphere from which iridescence is visible. We will refer to these portions of the hemisphere as ‘dark zones’ and a more detailed explanation will appear below.

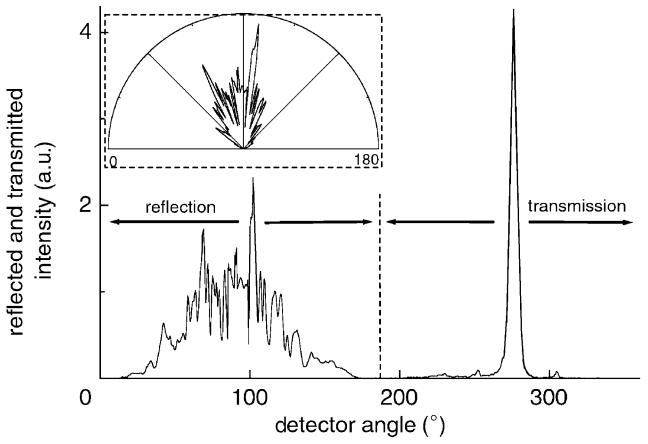

Figure 3. Reflection and transmission of 543 nm laser light from a single iridescent scale taken from region A of the ventral hind-wing of *A. meliboeus*. Incidence was normal to the plane of the scale (at the 90° point on the graph axis). Inset graph shows the reflection only, as a polar plot. (Note: although there appear to be two regions with minimal reflectivity in this polar plot, they are not associated with dark zones. They are produced by the near-collimated nature and normal incidence of the illuminating laser.)

In figure 1*a*, the wing is orientated in such a way that the camera is completely in a dark zone for region B. As the wing tilts, the camera's position increasingly moves out of this dark zone and region B iridesces blue. The final image in this sequence shows region B iridescing green; with further tilt it becomes yellow and follows an identical colour transition to that of region A.

Figure 2 is a photograph showing the reflection, onto a flat white screen, of a narrow collimated beam of white light incident normally on region A. This image is particularly interesting as it illustrates several features. First, the range of colours (from blue to yellow to orange) within the reflected band is visible. This range corresponds very closely to the colours shown in the images of figure 1. Second, there is a broad spread in reflectivity in one direction (horizontal in the photograph) compared to the other. The long axis of this broad spread runs perpendicularly to the direction of the ridges of the scales in this region. Such broadening in reflection (illustrated at the single-scale level in figure 3) from multilayers that make up the scale ridges (imaged in figure 4) has been observed previously in *Morpho* scales (Vukusic *et al.* 1999). It is attributed to the lateral 'leaning' of both the ridging and the multilayering within the ridging on the iridescent scales. The single-scale reflectivity and transmissivity data from figure 3 were collected in the plane running perpendicular to the line of scale ridges, where, for a *ca.* 5° convergence on the incident beam, the reflectivity diverges across almost 100°. No significant divergence is measured in the plane parallel to the ridging because there is little lateral spread in the tilt of the layering in this plane. Transmission data through this single scale is also collected and presented in figure 3. It shows low-intensity diffraction maxima to either side of the zero order peak. This diffraction can be quantifiably attributed to the periodicity of the ridges on the scale.

Using SEM and TEM images of iridescent scales from *A. meliboeus*, we found evidence that accounts for what we have termed the dark-zone effect. Its scale multilayering is similar to the multilayering present in iridescent *Morpho* butterfly scales (both *Morpho* and *A. meliboeus* are said to exhibit class I iridescent scales (Vukusic *et al.* 2000*a*)). In *A. meliboeus*, the ridging that runs the full length of each scale comprises between five and six layers of cuticle, separated by air spaces. By contrast, while the layering within

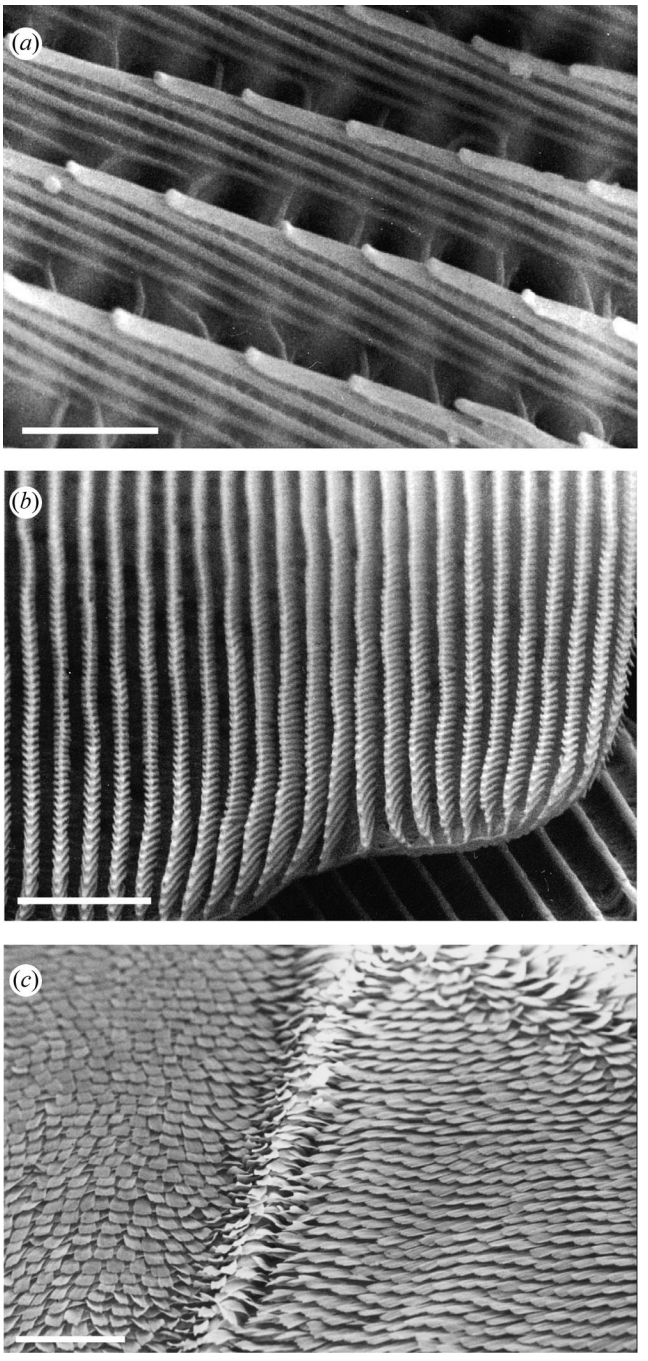

Figure 4. Electron microscopy of *A. meliboeus*. (*a*) Micrograph of a small region of iridescent scale showing a side profile of several multilayered ridges. (*b*) Micrograph of the end of an iridescent scale (the viewing direction tilted 60° from normal incidence) showing the structure of the ridges in a different perspective to that of image (*a*) and their relation to the outline of the scale. (*c*) Low-magnification image showing the different orientations of scales in neighbouring iridescent regions (the lines of ruffled scales outline the presence of wing veins). Scale bars, (*a*) 700 nm, (*b*) 3 μm, (*c*) 500 μm.

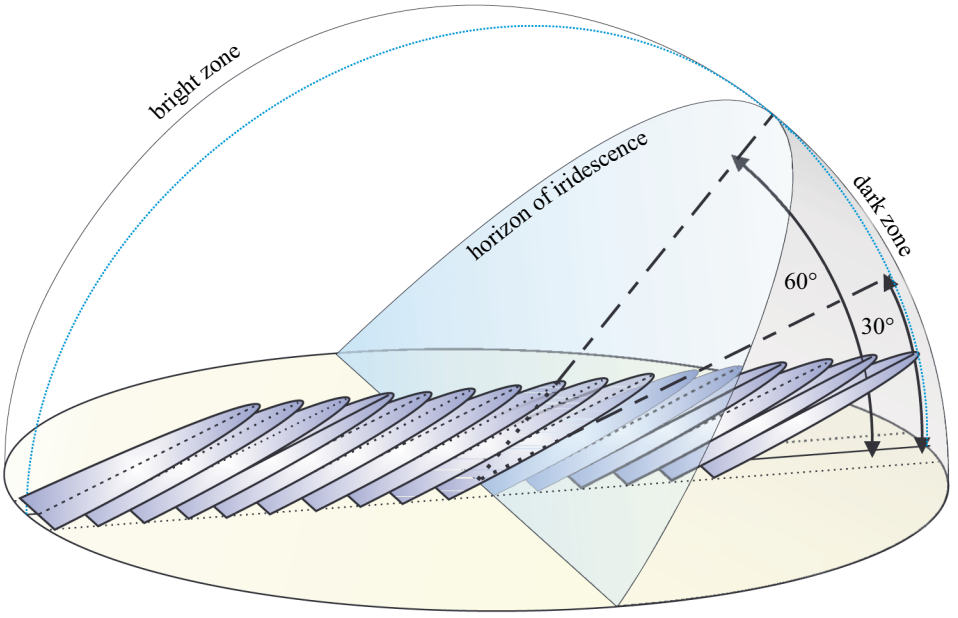

Figure 5. Schematic image showing the observation hemisphere and the existence of the bright and dark zones in relation to the tilt of the ridge multilayering of *A. meliboeus*. (Reprinted with permission from *Nature* (Vukusic *et al.* 2001) ©Macmillan Magazines Ltd.)

ridging on *Morpho* scales runs nearly parallel to the scale substrate (termed class Ia (Vukusic *et al.* 2000*a*)), the layering on *A. meliboeus* does not (figure 4). Its layering is inclined at *ca.* 30° to the scale substrate (described as class Ib (Vukusic *et al.* 2000*a*)). It is this difference that has the effect of introducing a 'dark zone' at one end of the ridges and, subsequently, the scales (figure 5). This dark zone is a 60° portion of the hemisphere above the wing from which an observer will see no iridescence from the scale and it is symmetrical across the longitudinal axis of the scale rather than along it. Reorientation of the wing (and therefore the scales), such that the observer's position is moved in or out of the dark zone of each wing, causes the iridescent colour to appear to flash on or off.

More subtle flashing effects, which appear to give neighbouring regions their contrasting colours, are created by small variations in scale orientations between these iridescent regions (figure 4*c*). Not only do these variations prevent the dark zones associated with each region from overlapping completely, but also they contribute to the observed colour differences between regions (figure 1).

(a) *Reciprocal lattice analysis*

To understand the mechanism for the production of such a broad range of colour from this multilayer, the effect brought about by the significant inclination of the multilayer within the ridging must be considered. It is this that causes strong periodicity at the top surface of the ridges where each layer terminates. Such surface periodicity contributes an additional diffraction consideration for light interacting with the structure; consequently, strongly reflected wavelengths must simultaneously satisfy both multilayer interference and diffraction conditions.

To effect a suitable analysis of this combined interference and diffraction effect, we follow a Ewald sphere treatment of the reciprocal space of the structure (Guinier 1963). Two orthogonal periodicities are identified. Referring to figure 6, the first is in the horizontal plane (x-direction) and results from the intersection of the multilayer with the scale surface (d_x). The second (d_y) is in the vertical plane (y-direction).

If the intrinsic periodicity running orthogonal to the layering itself is 'd', then d_x and d_y are given by

$$d_x = \frac{d}{\sin\alpha} \text{ and } d_y = \frac{d}{\cos\alpha}, \tag{3.1}$$

where α is the angle of inclination of the layering with respect to the horizontal plane.

This bi-periodicity in real space may be represented by reciprocal vectors (Guinier 1963) $\boldsymbol{G}_x$ and $\boldsymbol{G}_y$, where

$$\boldsymbol{G}_x = \frac{2\pi}{d_x} \text{ and } \boldsymbol{G}_y = \frac{2\pi}{d_y}. \tag{3.2}$$

These reciprocal vectors make up the reciprocal space lattice, because $\boldsymbol{G}_x$ and $\boldsymbol{G}_y$ are reciprocally related to the real space periodicities. However, care must be taken in the representation of the individual reciprocal lattice points. From Fourier analysis (Lipson & Lipson 1969), the mathematical function that predicts the scattered intensity from this and other periodic structures is shown to be proportional to Φ where

$$\Phi = \frac{\sin^2(NKd/2)}{\sin^2(Kd/2)}, \tag{3.3}$$

where d is the periodicity of the structure and k is the incident wave vector.

This expression is plotted in figure 7 for $N = 100$ (representing the minimum number of horizontal scatterers on the scale within the surface periodicity), and $N = 5$ (representing the number of vertical scatterers within the multilayer periodicity). The properties of this function are well documented (Lipson & Lipson 1969). The function is zero whenever the numerator is zero, except when the

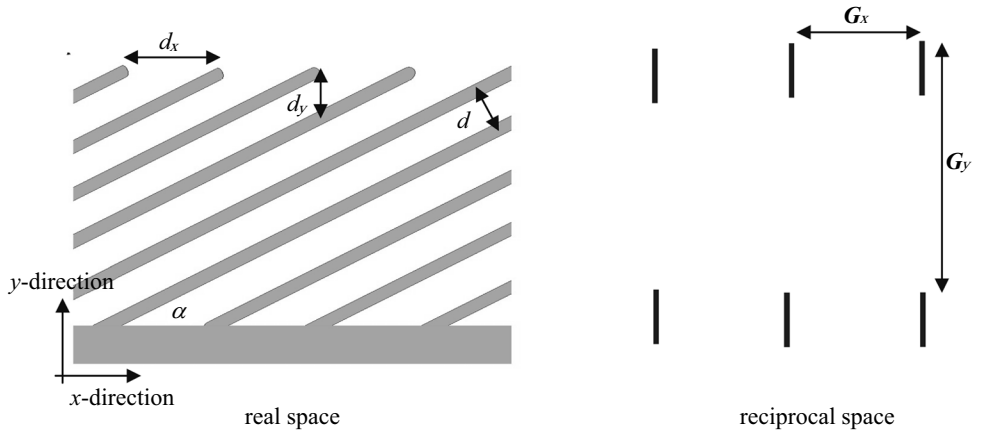

Figure 6. Schematic diagram of the real space and reciprocal space associated with an *A. meliboeus* iridescent scale. The real space diagram shows the cross-section through the long axis of a single ridge, while the reciprocal space diagram shows the corresponding distribution and elongation of reciprocal lattice points.

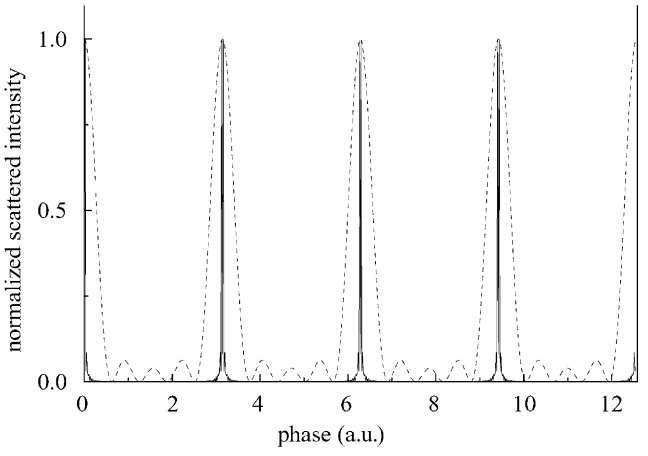

Figure 7. Graphical representation of the scattered intensity (proportional to the sine function in equation (3.3)) from $N = 5$ (dashed line) and $N = 100$ (solid line) periodic scatterers.

denominator is also zero; then it is N^2. When N is large, the principal maxima become outstanding compared to the subsidiary maxima. When N is very large, the maxima approximate to δ-functions. In the x-direction, along the periodic grating on the top surface of each ridge, there are in excess of 100 scatterers. Reciprocal space in this direction may therefore be treated as a set of δ-functions separated by $\boldsymbol{G}_x$.

However, in the y-direction (which incorporates the periodicity of the multilayer), there are as few as five scatterers due to the limited number of layers. This causes the resulting maxima of scattered intensity to be of finite width (i.e. they cannot be treated as δ-functions). In fact, the finesse of this system of $N = 5$ periods (defined as the ratio of full width at half maximum (FWHM) to the separation of maxima) approximates as $\boldsymbol{G}_y/5$. This provides a guide to the width of the scattering points in the reciprocal lattice. In this y-direction therefore, because the use of δ-functions is not appropriate, the reciprocal lattice may be represented as elongated points of width $\boldsymbol{G}_y/5$, whose centres are separated by $\boldsymbol{G}_y$.

The elongated grid points shown on the right of figure 6 represent the resulting reciprocal space based on the real space periodicities of the *A. meliboeus* scale structure in the x- and y-directions. These real space periodicities were taken directly from SEM and TEM analysis. This reciprocal lattice may now be used to define the scattering vectors that govern the interaction of light with the structure.

Consider incident radiation of wave vector $\boldsymbol{k}_0$ that is strongly scattered by the wing-scale structure to a new wave vector $\boldsymbol{k}_s$. In order to conserve energy, the incident and scattered waves must have the same frequency and therefore the magnitudes of $\boldsymbol{k}_s$ and $\boldsymbol{k}_0$ must be equal. This condition may be represented geometrically by saying that $\boldsymbol{k}_s$ and $\boldsymbol{k}_0$ must be radius vectors on the same circle (referred to as the Ewald sphere or reflecting sphere in three-dimensional situations).

To satisfy the additional condition of momentum conservation, the incident and scattered wave vectors must end on reciprocal lattice points. This necessarily implies that their difference, $\boldsymbol{k}_s - \boldsymbol{k}_0$, is an integer ($n$ and m) multiple of reciprocal lattice vectors ($n\boldsymbol{G}_x + m\boldsymbol{G}_y$) and is supplied by the periodicity of the reciprocal lattice.

To test the validity of this model, an analysis of incidence that is normal to the multilayers is conducted. In relation to the reciprocal lattice in figure 6, where the preferential scattering direction (Guinier 1963) is the −1,1 direction (from centre to centre of reciprocal lattice points), momentum conservation requires that

$$\boldsymbol{k}_s - \boldsymbol{k}_0 = -\boldsymbol{G}_x + \boldsymbol{G}_y. \tag{3.4}$$

Substituting for $\boldsymbol{G}_x$ and $\boldsymbol{G}_y$ from equations (3.1) and (3.2), and using the geometry of figure 8:

$$|\boldsymbol{k}_s - \boldsymbol{k}_0| = \frac{2\pi}{d}(\sin^2\alpha + \cos^2\alpha)^{0.5} = \frac{2\pi}{d}. \tag{3.5}$$

In the case of incidence that is normal to the multilayers, $\boldsymbol{k}_0 = -\boldsymbol{k}_s$ and, subsequently,

$$2\boldsymbol{k}_0 = \frac{2\pi}{d}, \tag{3.6}$$

giving

$$\lambda_0 = 2d. \tag{3.7}$$

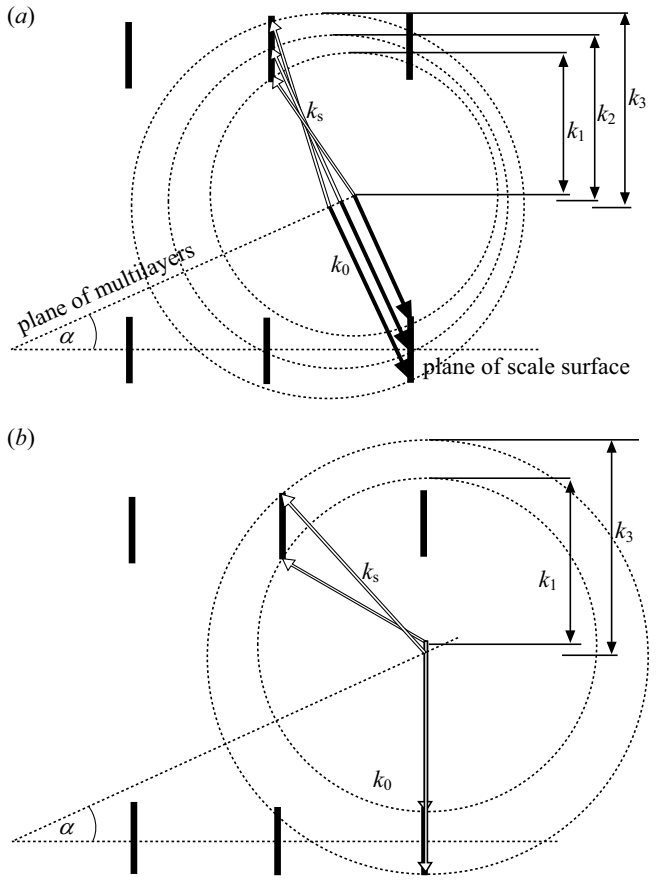

Figure 8. (*a*) Elongated grid points represent the reciprocal space of the *A. meliboeus* iridescent scale structure. $\boldsymbol{k}_0$ describes the incident wave vector and $\boldsymbol{k}_s$ the scattered wave vector for three different wavelengths (where $\lambda_1 = 2\pi/\boldsymbol{k}_1$, $\lambda_2 = 2\pi/\boldsymbol{k}_2$ and $\lambda_3 = 2\pi/\boldsymbol{k}_3$). Despite their incidence at the same angle, it is possible for the different wave vectors to be scattered in different directions. This is caused by simultaneous interference and diffraction, creating the broad colour effects observed in *A. meliboeus*. (*b*) This diagram represents scattering from the elongated reciprocal space points for incidence that is normal to the plane of the scale (centre-to-centre point scattering is not included.)

Thus, for incidence normal to the plane of the multilayer, strong reflection is produced for a wavelength that is twice the optical periodicity of the multilayer. This agrees with standard multilayer theory (Huxley 1968; Land 1972). Indeed the analysis proves consistent with standard multilayer theory at any angle of incidence.

The effect of the elongation of the reciprocal lattice points must now be considered. For collimated white light incident normal to the multilayers (similar to the illumination conditions used for figure 2), we find that a rather broad range of wavelengths can be scattered (see figure 1). In order for this to occur, however, the scattered directions for each wavelength must be different. Figure 8 illustrates that scattering between diagonally neighbouring reciprocal lattice points can occur at normal incidence, but that this scattering must be between distinct parts of each lattice point. The shortest wave vector $\boldsymbol{k}_1$ (which corresponds to the longest wavelength) may scatter from the top of one lattice point to the bottom of its diagonal neighbour. The longest wave vector $\boldsymbol{k}_3$ (shortest wavelength) may scatter, in the way shown, from the bottom of one reciprocal lattice point to the top of its diagonal neighbour. Notice, however, that although we have limited both wave vectors to normal incidence (which is the illumination condition), the directions of their respective scattered wave vectors are different; i.e. the wing scale exhibits different coloration at different positions in the bright zone of the observation hemisphere.

In this way, therefore, the elongation of reciprocal lattice points (that results from the limited number of multilayers and their tilt with respect to the plane of the scale) disperses incident white light. This phenomenon is not only limited to incidence that is normal to the multilayers. Figure 8*b* shows that it also holds for incidence normal to the scale substrate. In fact, it holds true for all angles of incidence but is most effective when incidence is normal to the multilayers.

More realistically, however, it is not the observer that moves across the observation hemisphere of the wing; it is the wing, while opening and closing, that creates the effect of moving its observation hemisphere across a stationary observer. Figure 9 represents this situation in reciprocal space. Wing movement effects rotation of reciprocal space: subsequently, when white light is incident from a specific direction, strong scattering in the observer's direction for different wing positions is only possible for distinct wavelengths. As wing movement displaces the observer towards normal incidence over the plane of the scale (an anti-clockwise rotation of reciprocal space in figure 9), the strongly scattered wave vector becomes larger; i.e shorter in wavelength. This is a reverse colour change compared to conventional multilayering, which strongly reflects longer wavelengths closer to normal incidence. It is an identical outcome to that represented in figure 8 and is a unique property of this system.

4. DISCUSSION

Dynamic stimuli were long believed to elicit a strong response in the visual systems of certain butterflies. Behavioural evidence has verified this (Magnus 1958), indicating that more and more effective super-normal stimuli may be created through an increase in the degree of flicker of a dummy's apparent motion, until the flicker fusion frequency of the butterfly's eye is reached (Magnus 1958). In studies of butterfly visual systems, not only have different temporal responses (Nakagawa & Eguchi 1994) been discovered in photoreceptors, but also these photoreceptors have been shown to have specific spectral characteristics that effect strong hue and intensity discrimination (Bernhard *et al.* 1970; Menzel 1979; Bandai *et al.* 1992). In some species, additional artifices, such as tapetal filter reflectors (Miller & Bernard 1968; Ribi 1980), further enhance the extent of colour and intensity discrimination. Therefore, with flicker, colour and colour contrast marked as important variables effecting conspecific visual stimuli in butterflies, how might selection pressures produce a mechanism that propitiates flashing and high contrast coloured signalling to optimize communication and visibility? In *A. meliboeus* we find a mechanism that, for several reasons, is uncommonly effective in these respects. First, microstructure, rather than pigmentation, is responsible

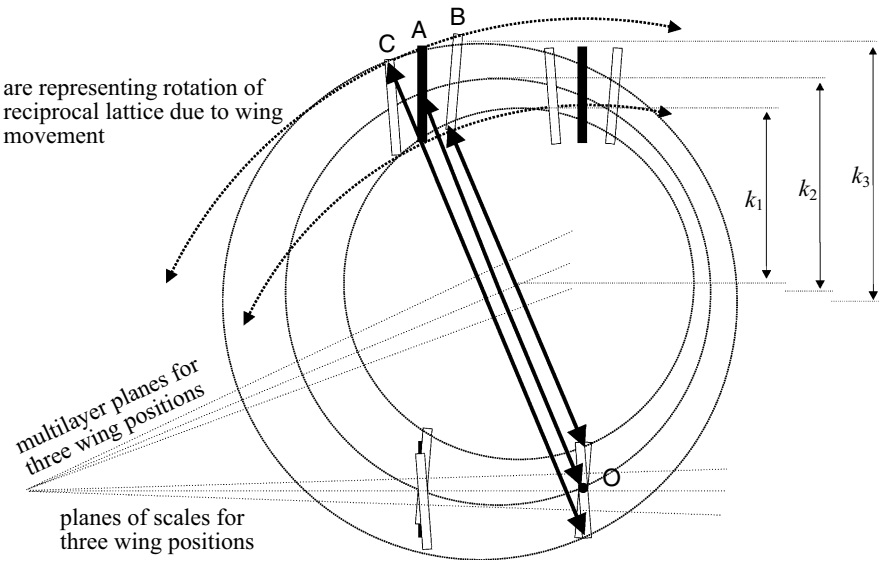

Figure 9. Reciprocal space of the *A. meliboeus* system showing strongly scattered wave vectors to a fixed observer as the wing moves (i.e. causing reciprocal space to rotate about the reciprocal lattice point labelled O). A is the reciprocal lattice point with no initial movement, while B and C represent the new positions of A after clockwise and anti-clockwise motion, respectively. Here, under conditions of fixed incidence and strong scattering directions, wing movement effects a reverse colour change in scattered angle, compared with conventional multilayering.

for its colour. This produces reflections of superior absolute brightness and higher spectral purity, thus effecting remarkable colour contrast. This is not unique to *A. meliboeus*, however, but is observed in many iridescent species (Vukusic *et al.* 2000*b*). *Ancyluris meliboeus* is rather more remarkable from the point of view of its abrupt intensity change with angle. This is effected through the tilt of the multilayering on its scales. Such tilt, of around 30° with respect to the plane of the scale, creates a 60° dark zone over the scale surface from which no structural coloration is visible. Very minor wing movements, even under completely diffuse illumination, may move an observer in or out of the scale's dark zone, providing high-contrast flicker signalling.

The nature of the multilayer tilt also contributes an additional effect. Where the multilayer intersects the top of the ridge, it produces a strong line of diffracting elements. These combine with the multilayering, in the way described earlier, to produce a uniquely broad range and transition of coloration with angle.

We observe too, that variations in orientation between different regions of scales across the wing surface further enhance the colour-dependent flicker. It has the effect of creating colour differences between regions on the wing, thereby increasing the range of colour flicker during wing movement.

Dorsal iridescent coloration, in the case of *Morpho* butterflies for example, is believed to be designed predominantly for signalling during flight (Silberglied 1984; Vukusic *et al.* 1999) and, to a lesser extent, for flashing signals upwards while at rest. By contrast, the ventral iridescence of *A. meliboeus*, due to the nature of the multilayer tilt on its scales, does not appear to be designed for in-flight signalling. In its natural rainforest habitat, even the brightest conditions of diffuse illumination and optimal signal–target position are calculated to effect poor in-flight reflectivity. This complexity of multilayer structure combined with the ultra-short duration in which the wing, while in flight, would be in an appropriate position to signal to a conspecific below it, render in-flight signalling unlikely as a design goal of this ventral iridescence.

It is suggested, therefore, that its ventral iridescence is principally designed for at-rest signalling. If *A. meliboeus* rests upright and horizontally, and starts with wings vertically together, a small wing movement down from vertical to horizontal will sweep multicoloured flashes across the areas below and to either side of it. Subsequent small upward wing movement will sweep the multicoloured signal back across the observer in the reverse direction and with reverse colour transition. Observations confirm that although *Ancyluris* species rest in a variety of positions depending on activity, males (typically defending territories) do perch along streamsides on top of leaves with their wings only very slightly open (i.e. closed over their backs and open *ca.* 10–20°), and occasionally they pulse their wings while walking over the substrate.

Detailed behavioural and visual system studies of *A. meliboeus* are necessary before firm conclusions can be made. With regard to the butterfly's visual system, measurement of flicker stimulus sensitivities and spectral characteristics of its photoreceptors may provide clues as to the selection pressures responsible for the development of its unique wing-scale structure.

The authors thank Gavin Wakely at the Electron Microscopy Unit, in the School of Biological Sciences of the University of Exeter for expert technical assistance, and Jason Hall of the Smithsonian Institute for help and information about *Ancyluris* butterfly behaviour. P.V. is funded by a BBSRC David Phillips Research Fellowship. Additional funding was provided by the University of Exeter and the Technology Group 08 of the Ministry of Defence Corporate Research Programme.

REFERENCES

Bandai, K., Arikawa, K. & Eguchi, E. 1992 Localization of spectral reflectors in the ommatidium of butterfly compound

eye determined by polarisation sensitivity. *J. Comp. Physiol.* A **171**, 289–297.
Bernhard, C. G., Boethius, J., Gemne, G. & Struwe, G. 1970 Eye ultrastructure, colour reception and behaviour. *Nature* **226**, 865–866.
DeVries, P. J. 1997 *The butterflies of Costa Rica and their natural history II. Riodinidae*. Princeton University Press.
Ghiradella, H. 1991 Light and colour on the wing: structural colours in butterflies and moths. *Appl. Optics* **30**, 3492–3500.
Ghiradella, H., Aneshansley, D., Eisner, T., Silbergleid, R. E. & Hinton, H. E. 1972 Ultra-violet reflection of a male butterfly: interference colour caused by thin layer elaboration of wing scales. *Science* **178**, 1214–1217.
Guinier, A. 1963 *X-ray diffraction*. San Francisco, CA: Freeman.
Huxley, A. F. 1968 A theoretical treatment of the reflection of light by multilayer structures. *J. Exp. Biol.* **48**, 227–245.
Huxley, J. 1975 The basis of structural colour variation in two species of *Papilio*. *J. Entomol.* A **50**, 9–22.
Land, M. F. 1972. The physics and biology of animal reflectors. *Prog. Biophys. Mol. Biol.* **24**, 75–106.
Lippert, W. & Gentil, K. 1959 Uber lamellare Feinstrukturen bei den Schillershuppen der Schmetterlinge vom Urania- und Morpho-typ. *Z. Morphol. Okol. Tiere* **48**, 115–122.
Lipson, S. G. & Lipson, H. 1969 *Optical physics*. Cambridge University Press.
Magnus, D. B. E. 1958. Experimental analysis of some 'over-optimal' sign-stimuli in the mating-behaviour of the fritillary butterfly *Argynnis paphia*. *Proc. Int. Congr. Ent.* **2**, 405–418.
Menzel, R. 1979 Spectral sensitivity and colour vision in invertebrates. In *Vision in invertebrates, handbook of sensory physiology*, vol. VII/6A (ed. H. Autrum), pp. 503–580. Berlin: Springer.
Miller, W. H. & Bernard, G. D. 1968 Butterfly glow. *J. Ultrastruct. Res.* **24**, 286–294.
Nakagawa, T. & Eguchi, E. 1994 Differences in flicker fusion frequencies of the five spectral photoreceptor types in the swallowtail butterfly's compound eye (RC). *Zool. Sci.* **11**, 759.
Ribi, W. A. 1980 The phenomenon of eye glow. *Endeavour* **5**, 2–7.
Silberglied, R. E. 1984 *The biology of butterflies*, *Symp. R. Soc. Lond.*, vol. 11 (ed. R. I. Vane-Wright & P. E. Ackery), pp. 207–223. London: Academic Press.
Vukusic, P., Sambles, J. R., Lawrence, C. R. & Wootton R. J. 1999 Quantified interference and diffraction in single *Morpho* butterfly scales. *Proc. R. Soc. Lond.* B **266**, 1403–1411.
Vukusic, P., Sambles, J. R. & Ghiradella, H. 2000*a* Optical classification of microstructure in butterfly wing-scales. *Photonics Sci. News* **6**, 61–66.
Vukusic, P., Sambles, J. R. & Lawrence, C. R. 2000*b* Structural colour: colour mixing in wing scales of a butterfly. *Nature* **404**, 457.
Vukusic, P., Sambles, J. R., Lawrence, C. R. & Wootton, R. J. 2001 Structural colour: now you see it—now you don't. *Nature* **410**, 36.

As this paper exceeds the maximum length normally permitted, the authors have agreed to contribute to production costs.